



**HAL**  
open science

# Optimal bacterial resource allocation strategies in batch processing

Agustín Gabriel Yabo, Jean-Baptiste Caillaud, Jean-Luc Gouzé

► **To cite this version:**

Agustín Gabriel Yabo, Jean-Baptiste Caillaud, Jean-Luc Gouzé. Optimal bacterial resource allocation strategies in batch processing. *SIAM Journal on Applied Mathematics*, 2024, pp.S567-S591. 10.1137/22M1506328 . hal-03710681v2

**HAL Id: hal-03710681**

**<https://inria.hal.science/hal-03710681v2>**

Submitted on 25 Sep 2023

**HAL** is a multi-disciplinary open access archive for the deposit and dissemination of scientific research documents, whether they are published or not. The documents may come from teaching and research institutions in France or abroad, or from public or private research centers.

L'archive ouverte pluridisciplinaire **HAL**, est destinée au dépôt et à la diffusion de documents scientifiques de niveau recherche, publiés ou non, émanant des établissements d'enseignement et de recherche français ou étrangers, des laboratoires publics ou privés.



Distributed under a Creative Commons Attribution 4.0 International License

# OPTIMAL BACTERIAL RESOURCE ALLOCATION STRATEGIES IN BATCH PROCESSING\*

AGUSTÍN GABRIEL YABO<sup>†</sup>, JEAN-BAPTISTE CAILLAU<sup>‡</sup>, AND JEAN-LUC GOUZÉ<sup>§</sup>

**Abstract.** The study of living microorganisms using resource allocation models has been key in elucidating natural behaviors of bacteria, by allowing allocation of microbial resources to be represented through optimal control strategies. The approach can also be applied to research in microbial cell factories, to investigate the optimal production of value-added compounds regulated by an external control. The latter is the subject of this paper, in which we study batch bioprocessing from a resource allocation perspective. Based on previous works, we propose a simple bacterial growth model accounting for the dynamics of the bioreactor and intracellular composition, and we analyze its asymptotic behavior and stability. Using optimization and optimal control theory, we study the production of biomass and metabolites of interest for infinite- and finite-time horizons. The resulting optimal control problems are studied using Pontryagin’s Maximum Principle and numerical methods, and the solutions found are characterized by the presence of Fuller phenomenon (producing an infinite set of switching points occurring in a finite-time window) at the junctions with a second-order singular arc. The approach, inspired in biotechnological engineering, aims to shed light upon the role of cellular composition and resource allocation during batch processing and, at the same time, poses very interesting and challenging mathematical problems.

**Key words.** mathematical systems theory; nonlinear systems; mathematical cell model dynamics and control; industrial biotechnology; optimal control; bacterial resource allocation

**MSC codes.** 37N25, 49K15, 92C42

**1. Introduction.** The study of living microorganisms through resource allocation models has become increasingly relevant for its capacity to elucidate natural behaviors of microbia through very simple dynamical models [7, 9, 12, 13, 21, 25]. The core idea is to represent the distribution of cellular resources through optimal control strategies, based on the assumption that evolutionary processes have tuned these endogenous allocation strategies to attain nearly-optimal levels [14]. Numerous problems arise in this context, one of them being the optimal production of metabolites regulated by an external control capable of arresting bacterial growth [11]. Growth control has proven a key engineering method for several industrial applications, such as in food preservation, biofuel production, and in combating antibiotics resistance [10]. To this end, a resource allocation approach can help understand how to modify the naturally-evolved allocation strategies so as to efficiently produce such chemical compounds [6].

These biosynthetic strategies have been studied in different frameworks. The simplest case describes the interactions between intracellular proteins with minimal interplay with the environment [27, 5, 22]. The latter can be modelled by omitting the dynamics of the substrate in the medium, representing the case where bacterial exponential growth can be attained. Another relevant, more complex case is continuous bioreactors [23, 26], used extensively in industries and in cell biology research for its capacity to reach and maintain steady-state growth conditions. The latter is

---

\*Submitted to the editors 30th June 2022.

**Funding:** This work was partially supported by ANR project Maximic (ANR-17-CE40-0024-01), Ctrl-AB (ANR-20-CE45-0014), Inria IPL Cosy and Labex SIGNALIFE (ANR-11-LABX-0028-01).

<sup>†</sup>MISTEA, Université Montpellier, INRAE, Institut Agro, Montpellier, France (agustin.yabo@inrae.fr, www.agustinyabo.com.ar)

<sup>‡</sup>Université Côte d’Azur, CNRS, Inria, LJAD, France (jean-baptiste.caillau@univ-cotedazur.fr)

<sup>§</sup>Université Côte d’Azur, Inria, INRAE, CNRS, Sorbonne Université, Macbes Team, Sophia Antipolis, France (jean-luc.gouze@inria.fr)

42 accomplished through an inflow of fresh medium rich in substrate and an outflow of  
43 the culture at the same volumetric flow rate, which produce a constant volume of the  
44 culture in the device. In that case, optimization studies are mostly oriented to reach  
45 such steady state in a cost-effective way. In fed-batch fermentation, the process starts  
46 with an initial volume of bacterial culture inside a bioreactor, which is progressively  
47 filled up through an inflow of rich medium, increasing the volume of the culture until  
48 it reaches a maximum level [24]. Once the maximum volume is attained, the culture  
49 evolves as a closed process, known in the field as batch processing. As no mass comes  
50 in or out of the device, the remainder of the nutrients in the medium are progressively  
51 consumed until the mass is entirely transformed into final products.

52 The latter is the subject of this paper, which tackles batch processing from a  
53 resource allocation perspective. The novelty of the approach lies in the nature of the  
54 model that—in addition to the physical and chemical laws found in classical biore-  
55 actor models—considers cellular composition, taking into account the intracellular  
56 components responsible for the main biological functions of bacteria. The problem  
57 has been first posed in [27], where a simpler mathematical model of resource alloca-  
58 tion is studied through numerical optimal control. The study does not consider the  
59 dynamical aspects of the model, neither the theoretical specifics arising from the opti-  
60 mal control problem and its singular arcs. We extend these results from an analytical  
61 perspective—both for the dynamical analysis and the optimal control study—and in-  
62 cluding the case with no metabolite synthesis as a starting point, which has not been  
63 analyzed in previous works. Based on simpler bacterial growth models [7, 25] that  
64 do not consider the dynamics of the substrate in the medium, a coarse-grained self-  
65 replicator model is introduced, including a heterologous pathway for the production of  
66 a value-added chemical compound [27, 22]. Additionally, the main biological assump-  
67 tions of the mechanistic bacterial model are revised, based on empirical studies of  
68 exponentially growing *E. coli* cultures [16]. Specifically, we consider a class of growth  
69 rate-independent proteins in the cellular composition that accounts for housekeeping  
70 proteins and non-active ribosomes, known to take up more than 50% of the cell [17].  
71 The inclusion of this class of proteins in previous models has shown considerable im-  
72 provement in the agreement between simulations and experimental data [25]. Using  
73 mass conservation laws related to the closeness of the bioprocess, it is possible to  
74 analyze the asymptotic behavior and stability of the dynamical system, showing that,  
75 for every possible allocation strategy, all component of the system are transformed  
76 either into proteins or into metabolites, a condition later defined as *Full depletion*.  
77 Then, two main studies are performed: the biomass maximization case, representing  
78 the natural objective of wild-type (i.e not modified) microbial cultures; and the me-  
79 tabolite maximization case, using the full bacterial model that includes the pathway  
80 for metabolite synthesis for industrial purposes. Both problems are analyzed in infi-  
81 nite time and in finite time, the latter stated as OCPs (Optimal Control Problems),  
82 which are investigated through the application of PMP (Pontryagin’s Maximum Prin-  
83 ciple) [15]. While the finite-time case is suitable for representing bioprocesses with  
84 predetermined duration, the analysis of the infinite-time case becomes crucial in un-  
85 derstanding the nature and asymptotic trend of the process. The solutions of the  
86 OCPs are characterized by the presence of Fuller’s phenomenon [3], producing arcs  
87 composed of an infinite set of switching points (*i.e.* bangs) over a finite-time window.  
88 These optimal solutions follow a Fuller-singular-Fuller structure, similar to the one  
89 found in [25], described by a single second-order singular arc which is delimited by  
90 two Fuller’s arcs at the beginning and at the end of the process. In particular, the  
91 solution of the biomass maximization case is thoroughly studied from an analytical

92 point of view, resulting in an explicit expression of the singular control in feedback  
 93 form. The results here presented are also confirmed by simulations obtained with  
 94 Bocop [18], an optimal control solver based on direct methods, and published in the  
 95 ct gallery<sup>1</sup> in order to guarantee the reproducibility of the numerical results.

96 The paper is organized as follows: in Section 2, the dynamical model is pre-  
 97 sented, and its dynamical behavior is studied in Section 3. The biomass and product  
 98 maximization cases are introduced and investigated in Sections 4 and 5, respectively.  
 99 Finally, the results are discussed in Section 6.

## 100 2. Model definition.

101 **2.1. Self-replicator model.** We define a self-replicator model describing the  
 102 dynamics of a microbial population growing inside a closed bioreactor. The bacterial  
 103 culture has constant volume  $\mathcal{V}_e$ , measured in liters. At the beginning of the experience,  
 104 there is an initial mass of substrate S inside the bioreactor, that is gradually consumed  
 105 by the bacterial population, and transformed into precursor metabolites P. These  
 106 precursors are intermediate metabolites used to produce proteins—such as ribosomes  
 107 and enzymes—responsible for specific cellular functions; and metabolites of interest  
 108 X which are excreted from the cell. The proteins forming bacterial cells are divided  
 109 into three classes M, R and Q, associated to the following cellular functions:

110 **Class M** Proteins of the metabolic machinery, responsible for the uptake of nutri-  
 111 ents S from the medium, the production of precursor metabolites P, and the  
 112 synthesis of metabolites of interest X.

113 **Class R** Proteins of the gene expression machinery (such as ribosomes) actively in-  
 114 volved in protein biosynthesis (*i.e.* in the production of proteins of classes M,  
 115 Q and R).

116 **Class Q** Growth rate-independent proteins, such as housekeeping proteins respon-  
 117 sible for cell maintenance, and ribosomes not involved in protein synthesis  
 118 [17].

119 From a biological perspective, the production of proteins M, R and Q is catalyzed by  
 120 ribosomal proteins R, and the absorption of S and synthesis of X are both catalyzed  
 121 by the metabolic proteins M. This catalytic effect is represented in Figure 1 through  
 122 dashed arrows. Intracellular proteins are produced at a synthesis rate  $V_R$  measured  
 123 in grams per hour. The synthesis rates of proteins M, R and Q are  $r_{\max}(1 - u)V_R$ ,  
 124  $r_{\max}uV_R$  and  $(1 - r_{\max})V_R$ , respectively; where the parameter  $r_{\max}$  is a certain em-  
 125 pirical constant imposing a maximum threshold to the rate of production of proteins  
 126 M and R. The proportion of precursors dedicated to the production of growth rate-  
 127 independent proteins Q is fixed, while the balance between proteins M and R is  
 128 decided by the allocation control  $u$ . The latter is modelled through a time-varying  
 129 function  $u(t) \in [0, 1]$ , where  $u = 0$  means no production of ribosomal proteins R, and  
 130  $u = 1$  means no production of metabolic proteins M. Depending on the objective to  
 131 be analyzed, the control  $u$  can represent different mechanisms. First, it can account  
 132 for the natural allocation used by bacteria, as modelled in [7, 25], by assuming that  
 133 the native regulatory mechanisms of bacterial cells have been tuned by the natural  
 134 selection to maximize growth rate. On the other hand, it can represent the artifi-  
 135 cially modified allocation modelled in [27]. In a biotechnological setting, the latter  
 136 is accomplished by engineering a synthetic growth switch that allows to modify the  
 137 natural allocation through external compounds like IPTG<sup>2</sup>.

<sup>1</sup>ct.gitlabpages.inria.fr/gallery/substrate/depletion.html

<sup>2</sup>Isopropyl  $\beta$ -D-1-thiogalactopyranoside

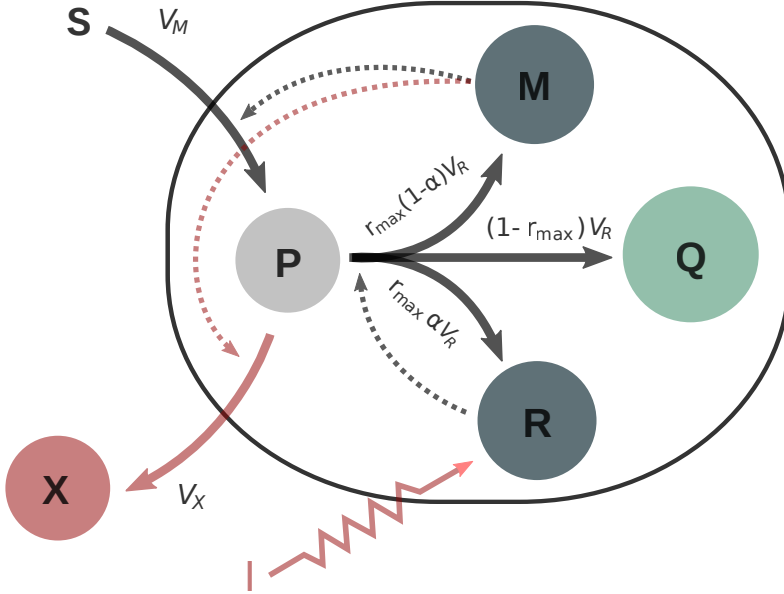


FIG. 1. *Self-replicator model of bacterial growth representing the intracellular micro-chemical reactions behind nutrient uptake, cell growth and metabolite synthesis. Solid arrows represent flow of resources resulting from the microchemical reactions, while dashed arrows indicate a catalyzing effect (i.e. the presence of a protein accelerating the synthesis of another protein).*

138 **2.2. Dynamical system.** The dynamics of the self-replicator system are de-  
 139 scribed by

$$\begin{cases} \dot{S} = -V_M, \\ \dot{P} = V_M - V_X - V_R, \\ \dot{R} = r_{\max} u V_R, \\ \dot{M} = r_{\max} (1 - u) V_R, \\ \dot{Q} = (1 - r_{\max}) V_R, \\ \dot{X} = V_X, \end{cases}$$

142 where the variables  $S(t)$ ,  $P(t)$ ,  $R(t)$ ,  $M(t)$ ,  $Q(t)$  and  $X(t)$  represent the masses (in  
 143 grams) of substrate, precursors metabolites, the gene expression machinery, the meta-  
 144 bolic machinery, the growth rate-independent proteins and the metabolites of interest  
 145 at time  $t$  measured in hours, respectively.  $V_M(t)$ ,  $V_R(t)$  and  $V_X(t)$  are the reaction  
 146 rates of the system (in grams per hour), and  $u(t)$  is the allocation control previously  
 147 defined. We define the volume (in liters) of the bacterial population in the bacterial  
 148 culture  $\mathcal{V}(t)$  as

$$(2.1) \quad \mathcal{V} \doteq \beta(M + R + Q),$$

151 where  $\beta$  is a constant relating protein density and volume [2]. Definition (2.1) pur-  
 152 posely neglects the mass of precursor metabolites  $P(t)$ , which greatly simplifies the  
 153 computations. The latter assumption is based on the fact that most of the mass in  
 154 bacterial cells corresponds to proteins of classes M, R and Q, as confirmed in previous

155 studies [7]. This allows to define time-varying intracellular concentrations (in grams  
156 per liter) with respect to this volume

$$157 \quad (2.2) \quad p \doteq \frac{P}{\mathcal{V}}, \quad r \doteq \frac{R}{\mathcal{V}}, \quad m \doteq \frac{M}{\mathcal{V}}, \quad q \doteq \frac{Q}{\mathcal{V}}.$$

159 Likewise, we define the extracellular concentrations related to the external volume

$$160 \quad (2.3) \quad s = \frac{S}{\mathcal{V}_e}, \quad x = \frac{X}{\mathcal{V}_e}.$$

162 We define the relative synthesis rates involved in the processes as increasing functions  
163 of the concentrations used in each reaction [17], and taking into account the catalytic  
164 effect previously described

$$165 \quad v_M(s, m) \doteq \frac{V_M}{\mathcal{V}}, \quad v_R(p, r) \doteq \frac{V_R}{\mathcal{V}}, \quad v_X(p, m) \doteq \frac{V_X}{\mathcal{V}}.$$

167 From (2.1) and (2.2), we have that

$$168 \quad (2.4) \quad m + r + q = \frac{1}{\beta},$$

170 which implies that the concentrations  $m$ ,  $r$  and  $q$  cannot be bigger than  $1/\beta$ . We  
171 define the growth rate of the bacterial culture  $\mu$  as

$$172 \quad \mu \doteq \frac{\dot{\mathcal{V}}}{\mathcal{V}} = \beta v_R(p, r).$$

174 Then, the dynamical system can be expressed in terms of the concentrations as

$$175 \quad \left\{ \begin{array}{l} \dot{s} = -v_M(s, m) \frac{\mathcal{V}}{\mathcal{V}_e}, \\ \dot{p} = v_M(s, m) - v_X(p, m) - v_R(p, r)(\beta p + 1), \\ \dot{r} = (r_{\max} u - \beta r) v_R(p, r), \\ \dot{m} = (r_{\max}(1 - u) - \beta m) v_R(p, r), \\ \dot{q} = ((1 - r_{\max}) - \beta q) v_R(p, r), \\ \dot{\mathcal{V}} = \beta v_R(p, r) \mathcal{V}, \\ \dot{x} = v_X(p, m) \frac{\mathcal{V}}{\mathcal{V}_e}. \end{array} \right.$$

177 **2.3. Kinetics definition.** We model the kinetics of the system by supposing  
178 that both the synthesis rates of precursors  $v_M$  and metabolites  $v_X$  are linear in the  
179 concentration of metabolic proteins  $m$ , and the protein synthesis rate  $v_R$  is linear in  
180 the concentration of active ribosomal proteins  $r$  [16]. Thus, they can be expressed as

$$181 \quad v_M(s, m) = w_M(s)m,$$

$$182 \quad v_R(p, r) = w_R(p)r,$$

$$183 \quad v_X(p, m) = \gamma w_R(p)m,$$

185 where  $\gamma > 0$  is a proportionality constant, which allows the metabolite synthesis  
 186 rate to be expressed as  $v_X(p, m) = \gamma v_R(p, r) m/r$ . Such assumption implies that  
 187 the bacterial cell has the same affinity to synthesize biomass and metabolites from  
 188 the precursors, even if the reactions do not consume P in the same proportion. In  
 189 the particular case of Michaelis-Menten kinetics, this feature is captured by the half-  
 190 saturation constant [8]. The functions  $w_I$  are assumed to have the following properties:

191 *Hypothesis 2.1.* Function  $w_I(x) : \mathbb{R}_+ \rightarrow \mathbb{R}_+$  is

- 192 • Continuously differentiable w.r.t.  $x$ ,
- 193 • Null at the origin:  $w_I(0) = 0$ ,
- 194 • Strictly monotonically increasing:  $w'_I(x) = \frac{\partial}{\partial x} w_I(x) > 0, \forall x \geq 0$ ,
- 195 • Strictly concave downwards:  $w''_I(x) = \frac{\partial^2}{\partial x^2} w_I(x) < 0, \forall x \geq 0$ ,
- 196 • Upper bounded:  $\lim_{x \rightarrow \infty} w_I(x) = k_I > 0$ .

197 For numerical simulations, we resort to the particular case where the functions follow  
 198 Michaelis-Menten kinetics. For that case, we define

$$199 \quad w_R(p) \doteq k_R \frac{p}{K_R + p}, \quad w_X(p) \doteq k_X \frac{p}{K_X + p}, \quad w_M(s) \doteq k_M \frac{s}{K_M + s},$$

201 where the values of the constants  $k_R, K_R, k_X, K_X, k_M$  and  $K_M$  are based on the  
 202 literature [7, 27]. For the general case introduced in Hypothesis 2.1, we define

$$203 \quad k_R \doteq \lim_{p \rightarrow \infty} w_R(p), \quad k_X \doteq \lim_{p \rightarrow \infty} w_X(p), \quad k_M \doteq \lim_{s \rightarrow \infty} w_M(s).$$

205 **2.4. Mass fraction formulation and non-dimensionalization.** We define  
 206 non-dimensional mass fractions

$$207 \quad (2.5) \quad \hat{s} \doteq \beta s, \quad \hat{p} \doteq \beta p, \quad \hat{r} \doteq \frac{\beta}{r_{\max}} r, \quad \hat{m} \doteq \frac{\beta}{r_{\max}} m, \quad \hat{q} \doteq \beta q, \quad \hat{x} \doteq \beta x,$$

209 where  $\hat{r}$  and  $\hat{m}$  are the mass fractions of the maximal ribosomal fraction  $r_{\max}$ . Then,  
 210 given that the transcription of housekeeping proteins in bacterial cells is internally  
 211 auto-regulated [20], and that the mass fraction of non-translating ribosomal proteins  
 212 is constant [16], we assume that the mass fraction of growth rate-independent proteins  
 213  $\hat{q}$  varies mildly compared to the remaining states, and thus we fix

$$214 \quad (2.6) \quad \hat{q} = 1 - r_{\max},$$

216 which, replacing in (2.4), yields

$$217 \quad \hat{m} + \hat{r} = 1.$$

219 The latter implies that the metabolic fraction can be expressed in terms of the ribosomal  
 220 fraction as  $\hat{m} = 1 - \hat{r}$ , and so the dynamical equation of  $\hat{m}$  can be removed from  
 221 the system. Additionally, we see that the quantity  $\beta r$  represents the mass fraction  
 222 of translating ribosomal proteins in the cell which, using (2.4) and (2.6), has bounds  
 223  $[0, r_{\max}]$ . Thus, its upper bound is given by the difference between the maximal total  
 224 ribosomal mass fraction and the constant non-translating ribosomal mass fraction. In  
 225 the literature [25], such values are empirically fixed to 0.5 and 0.07, respectively, and  
 226 so the parameter  $r_{\max}$  is here set to 0.43 for the numerical calculations. The biomass  
 227 fraction of the bacterial culture is defined as

$$228 \quad (2.7) \quad \hat{v} \doteq \frac{\mathcal{V}}{\mathcal{V}_e}.$$

230 We define the non-dimensional time  $\hat{t} \doteq k_R r_{\max} t$  and the non-dimensional functions

$$231 \quad \hat{w}_R(\hat{p}) = \frac{w_R(p)}{k_R}, \quad \hat{w}_X(\hat{p}) = \frac{w_X(p)}{k_R}, \quad \hat{w}_M(\hat{s}) = \frac{w_M(s)}{k_R}$$

233 so that  $\lim_{\hat{p} \rightarrow \infty} \hat{w}_R(\hat{p}) = 1$ . For the sake of simplicity, let us drop all hats from the  
234 current notation. Thus, the system becomes

$$235 \quad (\text{S}) \quad \begin{cases} \dot{s} = -w_M(s)(1-r)\mathcal{V}, \\ \dot{p} = w_M(s)(1-r) - \gamma w_R(p)(1-r) - w_R(p)r(p+1), \\ \dot{r} = (u-r)w_R(p)r, \\ \dot{\mathcal{V}} = w_R(p)r\mathcal{V}, \\ \dot{x} = \gamma w_R(p)(1-r)\mathcal{V}. \end{cases}$$

237 In this formulation, and using (2.2), (2.3), (2.4), (2.5) and (2.7), the total mass in the  
238 bioreactor can be expressed in terms of the concentrations as

$$239 \quad (2.8) \quad S + P + M + R + Q + X = \frac{\mathcal{V}_e}{\beta} (s + (p+1)\mathcal{V} + x).$$

### 241 3. Model analysis.

242 LEMMA 3.1. *The set*

$$243 \quad \Gamma = \{(s, p, r, \mathcal{V}, x) \in \mathbb{R}^5 : s \geq 0, p \geq 0, 1 \geq r \geq 0, \mathcal{V} \geq 0, x \geq 0\}$$

245 *is positively invariant for the initial value problem.*

246 Proving Lemma 3.1 is standard and can be done by evaluating the vector field of  
247 (S) over the boundaries of  $\Gamma$ . Thus, we fix initial conditions

$$248 \quad (\text{IC}) \quad \begin{aligned} s(0) &= s_0 > 0, & p(0) &= p_0 > 0, & x(0) &= 0, \\ r(0) &= r_0 \in (0, 1), & \mathcal{V}(0) &= \mathcal{V}_0 > 0, \end{aligned}$$

250 where the initial concentration of metabolites  $x(0)$  is set to 0 to represent the fact  
251 that, at the beginning of the bioprocess, no metabolite has been produced. Some  
252 relations are immediate from the dynamics: as  $\dot{s} \leq 0$  and  $\dot{\mathcal{V}} \geq 0$  for all  $t$ , we have

$$253 \quad (3.1) \quad s(t) \leq s_0, \quad \mathcal{V}(t) \geq \mathcal{V}_0,$$

255 representing the fact that the substrate can only be consumed (and not replenished),  
256 and the biomass can only grow.

257 **3.1. Total available mass.** As typically occurs in batch processes, there is  
258 neither inflow nor outflow of mass in the bioreactor, which is reflected in the dynamics  
259 of the system through a mass conservation law. We define the constant

$$260 \quad \Sigma \doteq s_0 + (p_0 + 1)\mathcal{V}_0,$$

representing the initial mass concentration in the system. It can be seen that the  
total mass concentration

$$z \doteq s + (p+1)\mathcal{V} + x$$



262 is constant for all  $t$  (as  $\dot{z} = 0$ ). This means that

$$263 \quad (3.2) \quad s + (p + 1)\mathcal{V} + x = \Sigma,$$

265 for all  $t$ . Thus, relation (2.8) and (3.2) show that the total mass in the system is  
 266 constant and equal to  $\mathcal{V}_e \Sigma / \beta$ . Variables  $\mathcal{V}$  and  $x$  are maximal when the remaining  
 267 variables are equal to 0, and so they are upper bounded. In particular, both  $\mathcal{V}(t)$  and  
 268  $x(t)$  are decreasing w.r.t.  $s(t)$  and  $p(t)$ . As neither  $s$  nor  $p$  can be negative, we have  
 269 that

$$270 \quad (3.3) \quad \mathcal{V}(t) + x(t) = \Sigma$$

272 when  $s(t) = p(t) = 0$ . This condition means that all the available substrate and pre-  
 273 cursor metabolites have been depleted and transformed into biomass and metabolites,  
 274 which is intuitively what one would expect from system (S) for  $t$  sufficiently large.  
 275 Additionally, using (3.1) and (3.2), we can obtain the following result.

276 **PROPOSITION 3.2.**  $\mathcal{V}(t) \in [\mathcal{V}_0, \Sigma]$ ,  $x(t) \in [0, \Sigma - \mathcal{V}_0]$  and  $p(t) \in [0, p^+]$  for all  $t$ ,  
 277 with  $p^+ = \Sigma / \mathcal{V}_0 - 1$ .

278 **3.2. Infinite-time full depletion.** Dynamics (S) shows that, under initial condi-  
 279 tions (IC),  $s(t)$  and  $p(t)$  can only vanish asymptotically, that is, when  $t \rightarrow \infty$ . The  
 280 latter can be proved by seeing that the derivatives of  $s$  and  $p$  can be bounded by

$$281 \quad \dot{s} \geq -w_M(s)\Sigma, \quad \dot{p} \geq -w_R(p)p^+(p^+ + 1 + \gamma),$$

283 which means that, at worst,  $s$  and  $p$  decay exponentially (as functions  $w_i(x)$  can be  
 284 upper bounded by linear functions  $w_i(x) \leq c_i x$ ), so that  $s(t) = p(t) = 0$  cannot be  
 285 reached in finite time. Accordingly, we define the depletion of  $s$  and  $p$  in an infinite-  
 286 time horizon.

287 **DEFINITION 3.3.** *System (S) achieves Full depletion when all the substrate and*  
 288 *the precursors are asymptotically depleted, i.e.*

$$289 \quad (\text{Full depletion}) \quad \lim_{t \rightarrow \infty} s(t) = \lim_{t \rightarrow \infty} p(t) = 0,$$

291 **3.3. Asymptotic behaviour.** Now, we study the system dynamics for an infi-  
 292 nite time  $t \rightarrow \infty$ . First, the case with a constant allocation  $u(t) = u^* \in (0, 1)$  for all  
 293  $t$  is analyzed, and then an extension to a general allocation function is proposed.

294 **3.3.1. Constant allocation  $u^*$ .**

295 **THEOREM 3.4.** *For any trajectory of system (S) with initial conditions (IC) and*  
 296 *constant allocation  $u(t) = u^*$ , it follows that*

$$297 \quad (3.4) \quad (u^* - r(t))\mathcal{V}(t) = (u^* - r_0)\mathcal{V}_0.$$

*Proof.* Under a constant allocation  $u(t) = u^*$ , the dynamics of  $r$  becomes

$$\dot{r} = (u^* - r)w_R(p)r.$$

Using dynamics (S), it is possible to see that both the total mass of proteins  $R = r\mathcal{V}$   
 and the quantity  $U = u^*\mathcal{V}$  have the same derivative

$$\dot{R} = \dot{U} = u^*w_R(p)r\mathcal{V},$$

299 which means that the difference of these two  $R_u = U - R$  should be constant (as  
 300  $\dot{R}_u = 0$ ), which yields (3.4).  $\square$

301 **3.3.2. General allocation**  $u(t)$ . Due to the boundedness of  $\mathcal{V}$  stated in Lemma 3.2,  $\blacksquare$   
 302 and the relation between  $\mathcal{V}$  and  $r$  shown in (3.2), we can see that any constant control  
 303  $u^*$  yields a bounded ribosomal fraction  $r$ . We extend this notion to any function  $u(t)$ .

304 **LEMMA 3.5.** *For any trajectory of system (S) with initial conditions (IC) and any*  
 305 *control  $u(t)$ , the ribosomal concentration has bounds  $r(t) \in [r^-, r^+]$  for all  $t$ , with*

$$306 \quad r^- \doteq r_0 \frac{\mathcal{V}_0}{\Sigma} > 0, \quad r^+ \doteq 1 - (1 - r_0) \frac{\mathcal{V}_0}{\Sigma} < 1.$$

308 *Proof.* Let us extend system (S) by defining variables  $r_{\text{low}}(t)$  and  $r_{\text{up}}(t)$  with  
 309 dynamics

$$310 \quad \begin{aligned} \dot{r}_{\text{low}} &= -r_{\text{low}} w_R(p) r \leq 0, & \dot{r}_{\text{up}} &= (1 - r_{\text{up}}) w_R(p) r \geq 0, \\ r_{\text{low}}(0) &= r_0, & r_{\text{up}}(0) &= r_0, \end{aligned}$$

which correspond to the dynamics of  $r$  with  $u = 0$  and  $u = 1$  respectively, and which satisfy

$$r_{\text{low}}(t) \leq r(t) \leq r_{\text{up}}(t)$$

for all  $t$ . The latter can be easily proved by showing that the time-varying differences

$$\Delta_{\text{low}}(t) = r(t) - r_{\text{low}}(t), \quad \Delta_{\text{up}}(t) = r_{\text{up}}(t) - r(t)$$

with dynamics

$$\dot{\Delta}_{\text{low}} = (u - \Delta_{\text{low}}) w_R(p) r, \quad \dot{\Delta}_{\text{up}} = (1 - u - \Delta_{\text{up}}) w_R(p) r$$

312 are always non-negative: they satisfy  $\Delta_{\text{low}}(0) = \Delta_{\text{up}}(0) = 0$  and are repulsive or  
 313 (at worst) invariant at 0. Then, based on the same principle used to obtain (3.4),  
 314 we define the quantities  $R_{\text{low}} = r_{\text{low}} \mathcal{V}$  and  $R_{\text{up}} = (1 - r_{\text{up}}) \mathcal{V}$  which are constant (as  
 315  $\dot{R}_{\text{low}} = \dot{R}_{\text{up}} = 0$ ), and so

$$316 \quad r_{\text{low}}(t) = r_0 \frac{\mathcal{V}_0}{\mathcal{V}(t)}, \quad r_{\text{up}}(t) = 1 - (1 - r_0) \frac{\mathcal{V}_0}{\mathcal{V}(t)},$$

318 for all  $t$ . As  $\mathcal{V}_0 \leq \mathcal{V}(t) \leq \Sigma$  for all  $t$ , we have

$$319 \quad r_{\text{low}}(t) \in \left[ r_0 \frac{\mathcal{V}_0}{\Sigma}, r_0 \right], \quad r_{\text{up}}(t) \in \left[ r_0, 1 - (1 - r_0) \frac{\mathcal{V}_0}{\Sigma} \right]$$

321 which shows that  $r^- \leq r(t) \leq r^+$  for all  $t$ .  $\square$

322 Lemma 3.5 states that, for any control  $u(t)$ , the ribosomal concentration never  
 323 reaches the bounds  $r = 0$  and  $r = 1$ , and thus neither the substrate intake nor the  
 324 protein synthesis is arrested. Using this fact, it can be proved that any control  $u(t)$   
 325 produces (*Full depletion*).

326 **THEOREM 3.6.** *Any trajectory of system (S) with initial conditions (IC) and any*  
 327 *control  $u(t)$  achieves (*Full depletion*) when  $t \rightarrow \infty$ .*

328 *Proof.* Using Lemma 3.5, it is easy to see that

$$329 \quad \dot{s} \leq -w_M(s)(1 - r^+) \mathcal{V}_0,$$

331 which means that  $s(t)$  converges to 0 as  $t \rightarrow \infty$ . Then, this means that

$$332 \quad \dot{p} \leq -\gamma w_R(p)(1 - r^+) - w_R(p) r^-,$$

334 and so  $p(t)$  also converges to 0 as  $t \rightarrow \infty$ .  $\square$

335 **4. The biomass maximization case.** In this section, we write the problem of  
 336 maximizing the biomass both for infinite time and finite time in terms of the alloca-  
 337 tion parameter  $u$ . The latter is a mathematical representation of the naturally-evolved  
 338 resource allocation strategy used by bacteria in nature. Indeed, in biology it is very of-  
 339 ten assumed that bacteria during exponential growth allocate their internal resources  
 340 to maximize their growth rate, thus maximizing long-term biomass production [7].  
 341 For this particular problem, we assume that no metabolite is produced, as the path-  
 342 way responsible for its production is artificially engineered, and thus not present in  
 343 wild-type bacteria. This is simply modeled through  $\gamma = 0$ . The resulting Wild-Type  
 344 Bacterial Model is

$$345 \quad (\text{WTB-M}) \quad \begin{cases} \dot{s} = -w_M(s)(1-r)\mathcal{V}, \\ \dot{p} = w_M(s)(1-r) - w_R(p)r(p+1), \\ \dot{r} = (u-r)w_R(p)r, \\ \dot{\mathcal{V}} = w_R(p)r\mathcal{V}, \end{cases}$$

#### 347 4.1. Infinite-time problem.

348 **4.1.1. Problem formulation.** We first write the biomass maximization prob-  
 349 lem for an infinite-time horizon, a non-realistic scenario that can provide valuable  
 350 insight into the finite-time process. Indeed, in this section, we show that the max-  
 351 imum attainable performance can only be achieved in infinite-time processes. The  
 352 problem can be expressed as

$$353 \quad \max_{u(t)} \lim_{t \rightarrow \infty} \mathcal{V}(t).$$

354 Since  $\mathcal{V} \in [\mathcal{V}_0, \Sigma]$ , applying (*Full depletion*) in (3.2) yields the condition

$$356 \quad \lim_{t \rightarrow \infty} \mathcal{V}(t) = \Sigma.$$

358 meaning that, in infinite time, the biomass is maximized for every control  $u(t)$ . We  
 359 formalize the latter in the following theorem.

360 **THEOREM 4.1.** *For any trajectory of system (WTB-M) with initial conditions*  
 361 *(IC) and any control  $u(t)$ , the volume  $\mathcal{V}(t) \rightarrow \max \mathcal{V}(t) = \Sigma$  as  $t \rightarrow \infty$ .*

362 As a consequence, using Theorem 3.4, we have the following result for constant  
 363 allocations.

364 **COROLLARY 4.2.** *For any trajectory of system (WTB-M) with initial conditions*  
 365 *(IC) and constant control  $u(t) = u^*$ ,*

$$366 \quad \lim_{t \rightarrow \infty} r(t) = u^* - (u^* - r_0) \frac{\mathcal{V}_0}{\Sigma}$$

368 These results are illustrated by the numerical simulations shown in next section.

369 **4.1.2. Numerical simulations.** Examples of trajectories confirming the ana-  
 370 lytical results are shown in Figure 2 and Figure 3, where we see that the system  
 371 approaches (*Full depletion*) asymptotically in every case, thus approaching the max-  
 372 imal biomass value  $\mathcal{V}(t) = \Sigma$ . Figure 2 shows the resulting trajectories associated to

373 the same initial conditions, when varying the allocation parameter  $u$ . On the other  
 374 hand, Figure 3 illustrates the trajectories for different values of  $r_0$ . Indeed, as  $\Sigma$  does  
 375 not depend on the resource allocation strategy, all the available mass is transformed  
 376 into biomass independently of the values of  $r_0$  and  $u(t)$ .

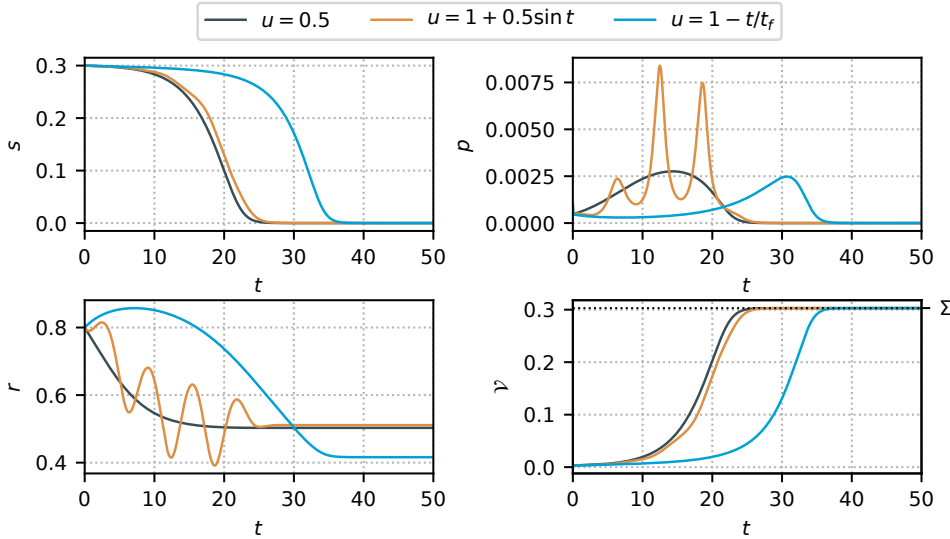


FIG. 2. Simulation of (WTB-M) with initial conditions  $s_0 = 0.3$ ,  $p_0 = 0.001$ ,  $r_0 = 0.8$ ,  $\mathcal{V}_0 = 0.003$ , fixed final time  $t_f = 50$  and different allocation functions  $u$ .

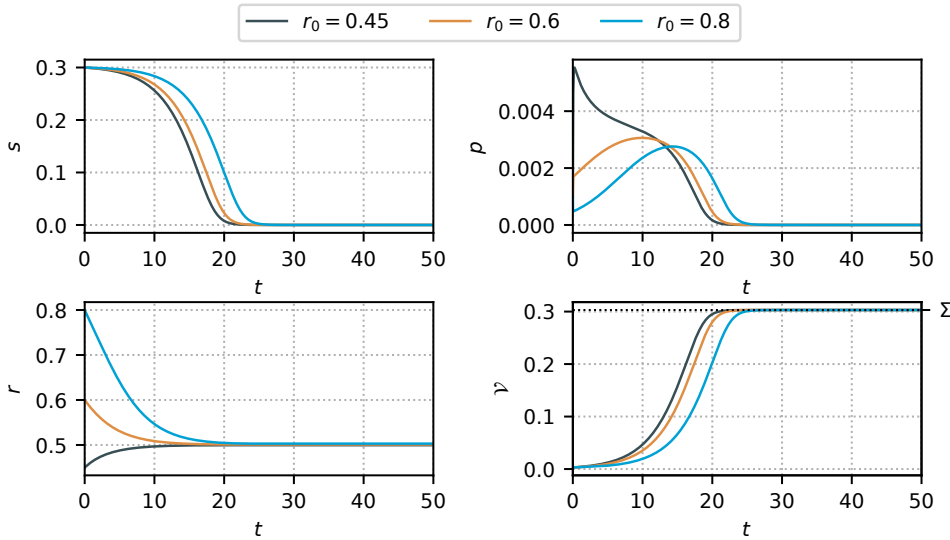


FIG. 3. Simulation of (WTB-M) with initial conditions  $s_0 = 0.3$ ,  $p_0 = 0.001$ ,  $\mathcal{V}_0 = 0.003$ ,  $u = 0.5$ , fixed final time  $t_f = 50$  and different values of  $r_0$ .

377

**4.2. Finite-time problem.**

378 **4.2.1. Problem formulation.** For the Biomass Maximization problem at final  
 379 time  $t_f$ , we write the OCP maximizing the final bacterial volume  $\mathcal{V}(t_f)$  with initial  
 380 conditions (IC):

$$381 \quad (\text{BM-OCP}) \quad \left\{ \begin{array}{l} \text{maximize} \quad \mathcal{V}(t_f), \\ \text{subject to} \quad \text{dynamics of (WTB-M)}, \\ \quad \quad \quad \text{initial conditions (IC)}, \\ \quad \quad \quad u(\cdot) \in \mathcal{U}. \end{array} \right.$$

382  
 383 For this class of optimal control problem, with no terminal constraints, there are no  
 384 controllability issues. Additionally, the dynamics is affine in the control, with the  
 385 latter included in a compact and convex set (a closed interval), and it can be checked  
 386 that every finite-time trajectory remains bounded. Thus, existence of a solution is  
 387 guaranteed by Filippov's theorem [1]. Then, for a problem (BM-OCP) with state  
 388  $\varphi \in \mathbb{R}^n$ , PMP ensures that there exists an absolutely continuous mapping  $\lambda(\cdot) : [0, t_f] \rightarrow \mathbb{R}^n$  such that the extremal  $(\varphi, \lambda, u)$  satisfies the generalized Hamiltonian system  
 390 system

$$391 \quad (\text{PMP}) \quad \left\{ \begin{array}{l} \dot{\varphi} = \frac{\partial}{\partial \lambda} H(\varphi, \lambda, u), \\ \dot{\lambda} = -\frac{\partial}{\partial \varphi} H(\varphi, \lambda, u), \\ H(\varphi, \lambda, u) = \max_{u \in [0,1]} H(\varphi, \lambda, u), \end{array} \right.$$

392  
 393 for almost every  $t \in [0, t_f]$ . We define the adjoint states for this particular case as  
 394  $\lambda = (\lambda_s, \lambda_p, \lambda_r, \lambda_v)$ , and we write the Hamiltonian

$$395 \quad H = -w_M(s)(1-r)\mathcal{V}\lambda_s + \left( w_M(s)(1-r) - w_R(p)r(p+1) \right) \lambda_p + w_R(p)r\mathcal{V}\lambda_v \\ 396 \quad + (u-r)w_R(p)r\lambda_r,$$

397  
 398 and the adjoint system as

$$399 \quad \left\{ \begin{array}{l} \dot{\lambda}_s = w'_M(s)(1-r)(\mathcal{V}\lambda_s - \lambda_p), \\ \dot{\lambda}_p = (w'_R(p)r(p+1) + w_R(p)r)\lambda_p - w'_R(p)r\mathcal{V}\lambda_v - (u-r)w'_R(p)r\lambda_r, \\ \dot{\lambda}_r = -w_M(s)(\mathcal{V}\lambda_s - \lambda_p) + w_R(p)((p+1)\lambda_p - \mathcal{V}\lambda_v) - (u-2r)w_R(p)\lambda_r, \\ \dot{\lambda}_v = w_M(s)(1-r)\lambda_s - w_R(p)r\lambda_v. \end{array} \right.$$

400  
 401 Given that there are no terminal conditions on the state, the transversality conditions  
 402 for the adjoint state are  $\lambda(t_f) = (0, 0, 0, 1)$ . Note that  $\lambda_v(t_f) = 1$  comes from the  
 403 fact that the cost function is  $\mathcal{V}(t_f)$  and there are no terminal conditions on the other  
 404 states (this prevents the so-called *abnormal* extremals with  $\lambda_v(t_f) = 0$ ). Since the  
 405 (WTB-M) dynamics is single-input and control-affine,

$$406 \quad \dot{\varphi} = F_0(\varphi) + uF_1(\varphi)$$

407 with obvious definitions for the vector fields  $F_0, F_1$ , the Hamiltonian writes  $H =$   
 408  $H_0 + uH_1$ . The Hamiltonian lifts  $H_i := \langle \lambda, F_i \rangle$ ,  $i = 0, 1$ , of the two vector fields are

$$409 \quad H_0 = -w_M(s)(1-r)\mathcal{V}\lambda_s + \left(w_M(s)(1-r) - w_R(p)r(p+1)\right)\lambda_p$$

$$410 \quad \quad \quad + w_R(p)r\mathcal{V}\lambda_V - w_R(p)r^2\lambda_r,$$

$$411 \quad H_1 = w_R(p)r\lambda_r.$$

413 The constrained optimal control  $u$  should maximize the Hamiltonian, so the solution  
 414 of (BM-OCP) is

$$415 \quad (4.1) \quad u(t) = \begin{cases} 0 & \text{if } H_1 < 0, \\ 1 & \text{if } H_1 > 0, \end{cases}$$

417 while  $u(t) = u_s(t)$  is called singular whenever  $H_1$  vanishes on a whole subinterval of  
 418  $[0, t_f]$ . This tells that an optimal control is a (possibly very complicated) concate-  
 419 nation of bangs ( $u = 0$  and  $u = 1$ ) and singular arcs, depending on the sign of the  
 420 switching function  $H_1$ . We see that, at final time, the dynamics of  $\lambda_r$  becomes

$$421 \quad \dot{\lambda}_r(t_f) = w_R(p(t_f))\mathcal{V}(t_f)\lambda_0 < 0,$$

423 which, using the fact that  $\lambda_r(t_f) = 0$ , implies that  $\lambda_r > 0$  for a period  $[t_f - \varepsilon, t_f]$ ,  
 424 and thus  $H_1 > 0$  for a period  $[t_f - \varepsilon, t_f]$ . As the control  $u$  should maximize the  
 425 Hamiltonian, we have the following result.

426 **LEMMA 4.3.** *There exists  $\varepsilon$  such that the final bang arc of the optimal control*  
 427 *solution of (BM-OCP) corresponds to  $u(t) = 0$  for the time interval  $[t_f - \varepsilon, t_f]$ .*

428 A more detailed analysis of the optimal control solution can be done by studying  
 429 the behavior of singular extremals. The latter is key in describing the structure of the  
 430 optimal control, as it is typically associated to intermediate values of the control  $u$   
 431 (i.e. non-bang arcs). In the general case application of PMP, the singular control can  
 432 be expressed as a function of the state and the adjoint state  $u_s(t) = f(\varphi, \lambda)$ , where the  
 433 explicit expression of  $f$  can be obtained by successively differentiating the switching  
 434 function  $H_1$  until the singular control can be solved for. In the next section, we show  
 435 for our problem that the singular optimal control is of order two, and that it can be  
 436 expressed in feedback form as  $u_s(t) = u(\varphi(t))$ . In control systems design, the latter is  
 437 a particular case that allows for a straightforward closed-loop implementation of the  
 438 optimal control law, and that can provide further insight on the nature of the optimal  
 439 trajectories.

440 **4.2.2. Singular arcs.** A singular arc occurs when  $H_1$  vanishes (as well as its  
 441 successive derivatives w.r.t. time) on a subinterval  $[t_1, t_2] \subset [0, t_f]$ , and so

$$442 \quad H_1 = w_R(p)r\lambda_r = 0,$$

444 As  $r$  is bounded and  $p$  cannot vanish in finite time, the condition becomes

$$445 \quad (4.2) \quad \lambda_r = 0.$$

447 We differentiate  $H_1$ , we evaluate the expression in (4.2), and we get

$$448 \quad \dot{H}_1 = w_R(p)r \left( -w_M(s)(\mathcal{V}\lambda_s - \lambda_p) + w_R(p)((p+1)\lambda_p - \mathcal{V}\lambda_V) \right) = 0.$$

450 Then, the Hamiltonian can be expressed as

$$451 \quad (4.3) \quad H = -w_M(s)(\mathcal{V}\lambda_s - \lambda_p) - r\lambda_r + (u - r)H_1 = c$$

on the interval  $[t_1, t_2]$ , where  $c$  is a positive constant that, due to the constancy of the Hamiltonian, is equal to

$$c \doteq H(t_f) = w_R(p(t_f))r(t_f)\mathcal{V}(t_f) > 0.$$

453 Then, (4.3) implies that, over a singular arc,

$$454 \quad (4.4) \quad w_M(s)(\mathcal{V}\lambda_s - \lambda_p) = w_R(p)((p+1)\lambda_p - \mathcal{V}\lambda_{\mathcal{V}}) = -c.$$

456 Differentiating  $\dot{H}_1$ , and evaluating over  $H_1 = \dot{H}_1 = 0$ , yields

$$\begin{aligned} 457 \quad \ddot{H}_1 &= w_R(p)r \left( w'_R(p)((p+1)\lambda_p - \mathcal{V}\lambda_{\mathcal{V}})(w_M(s)(1-r) - w_R(p)r(p+1)) \right. \\ 458 &\quad \left. + w_R(p)(w_M(s)(1-r) - w_R(p)r(p+1))\lambda_p \right. \\ 459 &\quad \left. + w_R(p)(p+1) \left( (w'_R(p)r(p+1) + w_R(p)r)\lambda_p - w'_R(p)r\mathcal{V}\lambda_{\mathcal{V}} \right) \right. \\ 460 &\quad \left. - w_R^2(p)r\mathcal{V}\lambda_{\mathcal{V}} - w_R(p)\mathcal{V}(w_M(s)(1-r)\lambda_s - w_R(p)r\lambda_{\mathcal{V}}) \right) = 0. \\ 461 \end{aligned}$$

462 By simplifying terms and replacing with (4.4), we obtain

$$463 \quad \ddot{H}_1 = cr(1-r) \left( w_R^2(p) - w'_R(p)w_M(s) \right) = 0.$$

465 which implies that

$$466 \quad (4.5) \quad \frac{w_R^2(p)}{w_M(s)w'_R(p)} = 1. \\ 467$$

468 The fact that  $u$  does not appear in  $\ddot{H}_1$  shows that any singular arc is at least of  
469 *local order two*, so that additional derivatives should be calculated in order to retrieve  
470 an explicit expression of the optimal control. Here, some precisions are in order,  
471 and we may first recall that the computation can also be performed in terms of  
472 Poisson brackets<sup>3</sup> since derivating along an extremal amounts to bracketing with the  
473 Hamiltonian. In particular,

$$\begin{aligned} 474 \quad \dot{H}_1 &= \{H_0 + uH_1, H_1\}, \\ 475 &= \{H_0, H_1\} =: H_{01}. \end{aligned}$$

477 Iterating, and with obvious notations ( $H_{001} := \{H_0, \{H_0, H_1\}\}$ , *etc.*), one obtains

$$478 \quad 0 = \dot{H}_{01} = H_{001} + uH_{101}.$$

479 (Let us recall that  $H_{01}$  is also equal to the Hamiltonian lift of the Lie bracket  
480  $[F_0, F_1] =: F_{01}$ , that  $H_{001}$  is the lift of  $[F_0, [F_0, F_1]] =: F_{001}$ , *etc.*) The previous  
481 computation shows that  $H_{101}$  is zero on the subset  $\{H_1 = H_{01} = 0\}$  of the cotangent  
482 space. These two relations have indeed been used during the computation, while an

<sup>3</sup>In coordinates, if  $fg$  and  $g$  are two scalar valued functions of  $(\varphi, \lambda) \in \mathbb{R}^{2n}$ ,  $\{f, g\} = \sum_{i=1}^n (\partial f / \partial \lambda_i)(\partial g / \partial \varphi_i) - (\partial f / \partial \varphi_i)(\partial g / \partial \lambda_i)$ .

483 explicit evaluation<sup>4</sup> allows to verify that the bracket  $H_{101}$  is *not* identically zero on  
 484 the whole cotangent space. In such a situation, the *local* (not *intrinsic*) order is said  
 485 to be at least two; that is at least two more differentiations *wrt.* time are required to  
 486 retrieve the singular control. We are actually in the following case (see also [4] for a  
 487 similar analysis):

488 PROPOSITION 4.4. *If the Lie bracket  $F_{101}$  belongs to the span of  $F_1$  and  $F_{01}$ , then*  
 489 *singular extremals must be of (local) order at least two.*

490 *Proof.* By assumption, if for some  $\varphi$  a covector  $\lambda$  is orthogonal to  $F_1$  and  $F_{01}$  at  
 491  $\varphi$ , it is also orthogonal to  $F_{101}$  at this point. So, along a singular extremal that must  
 492 belong to  $\{H_1 = H_{01} = 0\}$ , one has

$$493 \quad 0 \equiv H_{001} + u_s H_{101}$$

494 with  $H_{101}$  also vanishing. As a result,  $0 \equiv H_{001}$  along the singular, and one can  
 495 differentiate again:

$$496 \quad 0 \equiv H_{0001} + u_s H_{1001}.$$

497 Now, by Leibniz rule

$$498 \quad H_{1001} = \{H_1, \{H_0, H_{01}\}\} = \underbrace{\{-H_{01}, H_{01}\}}_{=0} + \{H_0, H_{101}\}$$

499 and there exist smooth functions  $a$  and  $b$  of  $\varphi$  such that  $F_{101} = aF_1 + bF_{01}$  (and  
 500 similarly for the associated Hamiltonian lifts). By Leibniz rule again,  $H_{1001}$  must  
 501 vanish when  $H_1 = H_{01} = H_{001} = 0$  as

$$502 \quad \{H_0, aH_1 + bH_{01}\} = \{H_0, a\}H_1 + aH_{01} + \{H_0, b\}H_{01} + bH_{001},$$

503 so  $H_{0001} \equiv 0$ . So one has to differentiate at least once more to retrieve the control.  $\square$

504 It should moreover be noted that  $\ddot{H}_1$  depends only on the state—and not on the  
 505 adjoint state—which implies that its successive derivatives also depend only on the  
 506 state, as the adjoint state does not appear in system (WTB-M). Additionally, and  
 507 based on Hypothesis (2.1), the function  $w_M(s)$  is invertible, which means that  $s$  can  
 508 be expressed in terms of  $p$  through equation (4.5). Once again, we differentiate  $\dot{H}_1$ ,  
 509 we evaluate over  $H_1 = \dot{H}_1 = \ddot{H}_1 = 0$ , and we get

$$510 \quad \begin{aligned} \ddot{H}_1 = c(1-r)r & \left( 2w_R(p)w'_R(p)(w_M(s)(1-r) - w_R(p)r(p+1)) \right. \\ 511 & \quad \left. - w''_R(p)w_M(s)(w_M(s)(1-r) - w_R(p)r(p+1)) \right. \\ 512 & \quad \left. + w'_R(p)w'_M(s)w_M(s)(1-r)\mathcal{V} \right) = 0. \\ 513 \end{aligned}$$

514 By rearranging the expression, we can express

$$515 \quad \ddot{H}_1 = c(1-r)r(\omega_0(p, \mathcal{V}) - \omega_1(p, \mathcal{V})r) = 0,$$

<sup>4</sup>Take for instance  $k_R = 1.1$ ,  $k_M = 1.2$ ,  $K_R = 1.3$ ,  $K_M = 1.4$ ,  $\varphi = \lambda = (1, 1, 1, 1)$  and check that  $H_{101}(\varphi, \lambda) \neq 0$ .



517 with

$$518 \quad \omega_0(p, \mathcal{V}) = w_M(s) \left( 2w_R(p)w'_R(p) - w''_R(p)w_M(s) + w'_R(p)w'_M(s)\mathcal{V} \right) > 0,$$

$$519 \quad \omega_1(p, \mathcal{V}) = \omega_0(p, \mathcal{V}) + w_R(p)(p+1)(2w'_R(p)w_R(p) - w''_R(p)w_M(s)) > 0,$$

521 where the positivity of functions  $\omega_i$  is a consequence of Hypothesis 2.1. The latter  
522 shows that, along the singular arc,  $r$  can be expressed in terms of  $p$  and  $\mathcal{V}$  (as, using  
523 (4.5),  $s$  can be expressed in terms of  $p$ ) as

$$524 \quad r = \frac{\omega_0(p, \mathcal{V})}{\omega_1(p, \mathcal{V})}.$$

526 Then, computing the next derivative and evaluating over the obtained conditions  
527 yields

$$528 \quad (4.6) \quad \ddot{H}_1 = c(1-r)r(\dot{\omega}_0(p, \mathcal{V}) - \dot{\omega}_1(p, \mathcal{V})r - \omega_1(p, \mathcal{V})(u-r)w_R(p)r) = 0.$$

530 We can see that the factor of  $u$  in expression (4.6) satisfies

$$531 \quad (4.7) \quad \frac{\partial}{\partial u} \ddot{H}_1 = -c(1-r)w_R(p)r^2\omega_1(p, s, \mathcal{V}) < 0$$

533 as  $\omega_1 > 0$  for all  $t$ , which leads to the following result.

534 **THEOREM 4.5.** *The singular optimal control is exactly of order two, and it can be*  
535 *expressed in feedback form,  $u = u(p, \mathcal{V})$ .*

536 *Proof.* Since it has been already proven that the singular arc is at least of order  
537 two, it suffices to prove that it cannot be of greater order. This can be done by  
538 observing that (4.7) cannot vanish. Thus, the singular arc is exactly of order two.  
539 Additionally, solving for  $u$  in the same expression yields

$$540 \quad u_s(p, \mathcal{V}) = \frac{\dot{\omega}_0(p, \mathcal{V}) - \dot{\omega}_1(p, \mathcal{V})r}{\omega_1(p, \mathcal{V})w_R(p)r} + r.$$

542 which shows that the control  $u$  can be expressed as a function of the state variables.□

543 We note that the generalized Legendre-Clebsch condition, necessary for optimality of  
544 the singular arc, is fulfilled in strict form by virtue of (4.7):

$$545 \quad (-1)^k \frac{\partial}{\partial u} \left( \frac{d^{2k}}{dt^{2k}} H_1 \right) = \frac{\partial}{\partial u} \ddot{H}_1 < 0.$$

547 **4.2.3. Numerical simulations.** The optimal trajectories were computed with  
548 Bocop [18], which solves the OCP through a direct method. The time discretization  
549 algorithm used is Lobato IIIC (implicit, 4-stage, order 6) with 2000 time steps. Figures  
550 4 and 5 show optimal trajectories for the same set of initial conditions and different  
551 values of  $t_f$ . Using the mass conservation law (3.2), the quantities are represented in  
552 the plots as fractions of the total mass in the bioreactor  $\mathcal{V}_e\Sigma/\beta$ . The optimal control  
553  $u$  is characterized by the presence of chattering after and before the singular arc, as  
554 expected in singular arcs of order two. From a biological point of view, both allocation  
555 strategies prioritize the synthesis of proteins of the metabolic machinery M (red in  
556 both Figures): the singular arc takes rather small values, and a large proportion of  
557 the optimal control corresponds to a bang arc  $u = 0$  at the end of the bioprocess.

558 The latter strategy promotes nutrient uptake, which results in a faster depletion of  
 559 the substrate. It is interesting to note that, in opposition to previous results in the  
 560 literature [7, 25], the presence of the turnpike properties [19] is not assured. Intuitively,  
 561 the turnpike phenomenon would cause the time interval corresponding to the singular  
 562 arc to increase as the final time  $t_f$  increases. However, a quick comparison between  
 563 Figures 4 and 5 shows that this is not the case, as the increase of  $t_f$  only produces  
 564 a larger 0-bang arc at the end of the bioprocess. This suggests that the duration  
 565 of the initial phase dedicating a fraction of the resources to ribosomal proteins is  
 566 fixed and independent of the duration of the batch process. Figure 6 also shows an  
 567 optimal trajectory, but with a different initial ribosomal concentration. According  
 568 to multiple simulations, this change shows an impact on the initial Fuller arc, that  
 569 becomes perceptively larger, but has no major effects on the remaining of the process.  
 570 Additionally, we note that the concentration of precursor metabolites in the bioreactor  
 571 remains negligible in comparison with the other quantities, a result that matches the  
 biological assumptions done in the modelling section.

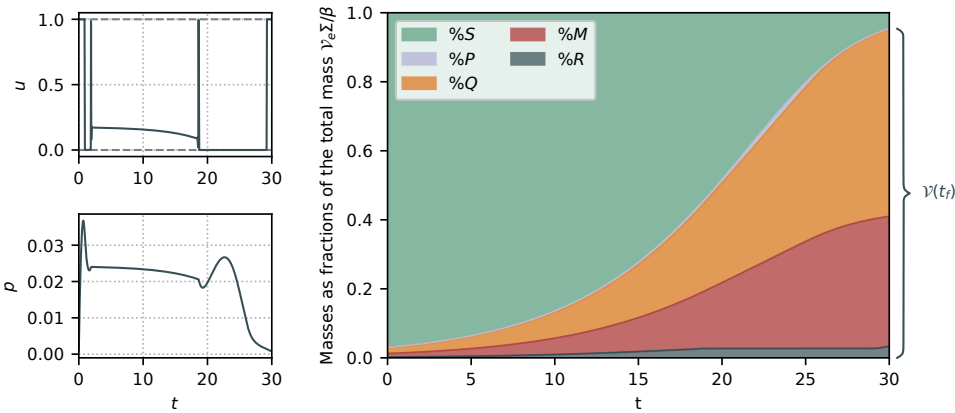


FIG. 4. Numerical simulation of (BM-OCP) with initial conditions  $s_0 = 0.1$ ,  $p_0 = 0.001$ ,  $r_0 = 0.1$ ,  $V_0 = 0.003$  and  $t_f = 30$ . Quantities in the right plot are shown as fractions of the total mass in the bioreactor  $V_e \Sigma / \beta$ . The final volume  $V(t_f)$  is at 95% of  $V_e \Sigma / \beta$ .

572

573

Figure 7 illustrates optimal trajectories in the  $sp$ -plane for different final times  
 574 (20, 25, 30 and 40). Each trajectory approaches the singular curve  $\dot{H}_1 = 0$  given  
 575 by expression (4.5) (obtained from the singular surface) through a Fuller arc, slides  
 576 along it during a certain time interval, and then follows a trajectory obtained from  
 577 the  $u = 0$  arc that approaches asymptotically (*Full depletion*). Naturally, the longer  
 578 the simulation of the process, the closer the final state to (*Full depletion*). These  
 579 results also confirm the observations previously done: the duration in time of the  
 580 singular arc is not directly related to the final time  $t_f$ . In fact, all the singular  
 581 arcs start at approximately the same time instant and finish around  $t = 18$ . The  
 582 independence of the initial phase from the duration of the bioprocess is coherent with  
 583 the fact that bacteria allocate resources in terms of their cellular composition and the  
 584 environment [7] (which, in this case, is described by the concentration of substrate in  
 585 the medium), independently of the man-made notion of duration of the bioprocess. It  
 586 is also noteworthy that, while the processes exit the singular surface at similar times,  
 587 the trajectories differ significantly as they exit the singular arc from different initial  
 588 conditions (not only in the  $(s, p)$  plane but also in the original  $\mathbb{R}^4$  space).

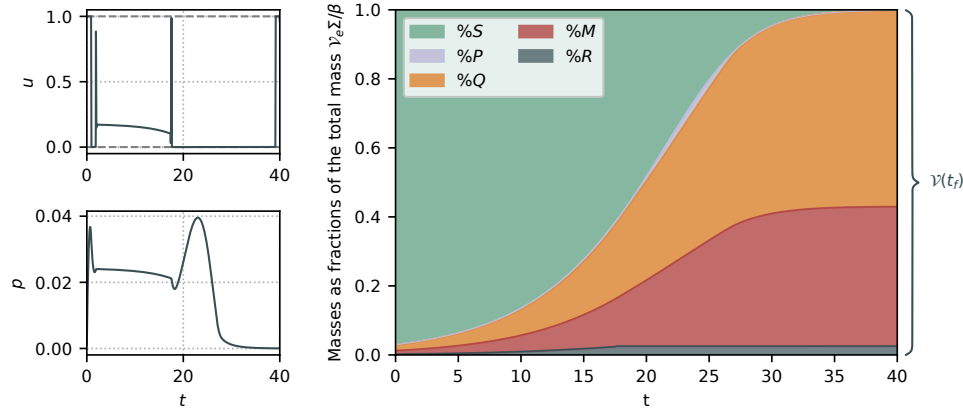


FIG. 5. Numerical simulation of (BM-OCP) with initial conditions  $s_0 = 0.1$ ,  $p_0 = 0.001$ ,  $r_0 = 0.1$ ,  $\mathcal{V}_0 = 0.003$  and  $t_f = 40$ . Quantities in the right plot are shown as fractions of the total mass in the bioreactor  $\mathcal{V}_e \Sigma / \beta$ . The final volume  $\mathcal{V}(t_f)$  is at 99.8% of  $\mathcal{V}_e \Sigma / \beta$ .

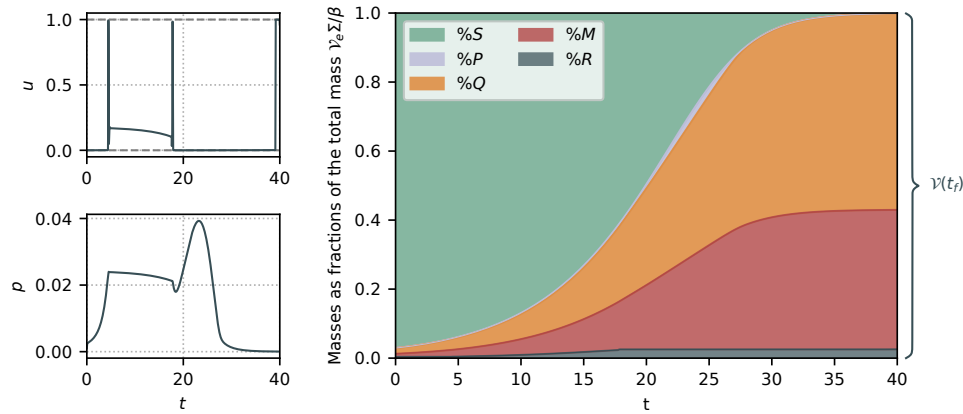


FIG. 6. Numerical simulation of (BM-OCP) with initial conditions  $s_0 = 0.1$ ,  $p_0 = 0.001$ ,  $r_0 = 0.3$ ,  $\mathcal{V}_0 = 0.003$  and  $t_f = 40$ . Quantities in the right plot are shown as fractions of the total mass in the bioreactor  $\mathcal{V}_e \Sigma / \beta$ . The final volume  $\mathcal{V}(t_f)$  is at 99.8% of  $\mathcal{V}_e \Sigma / \beta$ .

#### 4.2.4. Alternative approach: prescribed performance in minimum time. ■

589

590 As confirmed by the finite-time case studied in the last section, the associated opti-  
 591 mal control problem with fixed final time yields a final volume  $\mathcal{V}(t_f)$  that can be  
 592 viewed as a fraction (between 0 and 1) of the total mass concentration in the system  
 593  $\Sigma$ . Indeed, Theorem 4.1 showed that  $\mathcal{V}$  can reach its maximum value  $\Sigma$  only when  
 594  $t$  goes to infinity. Thus, (BM-OCP) can be reformulated to achieve a minimal-time  
 595 transfer between an initial state (IC) (with biomass  $\mathcal{V}(0) = \mathcal{V}_0$ ) and a final state with  
 596 terminal constraint

597 (TC)

$$\mathcal{V}(t_f) = \eta \Sigma,$$

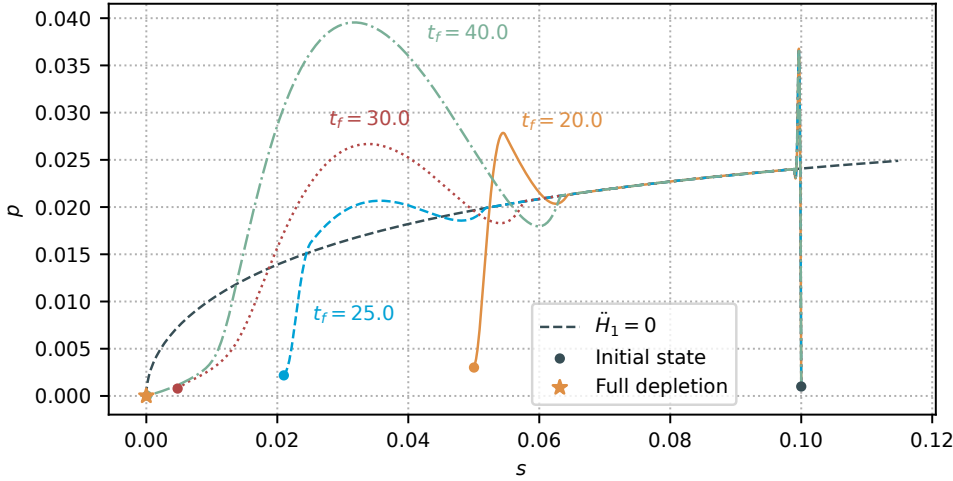


FIG. 7. Numerical simulation of (BM-OCP) showing different trajectories in the  $sp$ -plane. Initial conditions are set to  $s_0 = 0.1$ ,  $p_0 = 0.001$ ,  $r_0 = 0.1$ ,  $\mathcal{V}_0 = 0.003$ . In all cases, the state approaches the singular curve  $\dot{H}_1 = 0$  and slides along it.

599 for a certain performance parameter  $\eta \in [\eta_{\min}, 1)$ , where  $\eta_{\min} \doteq \mathcal{V}_0/\Sigma$ . The reformu-  
 600 lated minimal-time OCP with Prescribed Performance writes

$$\begin{cases}
 \text{minimize} & t_f, \\
 \text{subject to} & \text{dynamics of (WTB-M),} \\
 & \text{initial conditions (IC),} \\
 & \text{terminal constraints (TC),} \\
 & u(\cdot) \in \mathcal{U}.
 \end{cases}$$

601 (PP-OCP)

602

603 A natural question arising from OCPs with terminal constraints is the existence of a  
 604 solution. In this case, Theorem 4.1 guarantees that any final volume  $\mathcal{V}(t_f) = \eta\Sigma$  can  
 605 be reached in finite time, as long as  $\eta \in [\eta_{\min}, 1)$ . The latter ensures the existence of  
 606 the solution for any  $\eta \in [\eta_{\min}, 1)$ . The study of the solutions of (PP-OCP) can  
 607 be performed through an analogous PMP approach, with the difference that the  
 608 Hamiltonian is null for every  $t \in [0, t_f]$  due to the free final time  $t_f$ , and that there  
 609 is no terminal constraint on  $\lambda_{\mathcal{V}}$  (*i.e.*  $\lambda_{\mathcal{V}}(t_f)$  is free). Given the similarity with the  
 610 previously analyzed case, the computations of such optimal control solution are not  
 611 explicated here. A numerical solution of the problem is shown in Figure 8.

612 **5. The product maximization case.** As done in the previous section, we  
 613 approach the product maximization objective in infinite time and finite time using  
 614 the full model (S) where  $\gamma \in \mathbb{R}^+$ .

615 **5.1. Infinite-time problem.** The problem of maximizing the product concen-  
 616 tration at infinite time is given by the expression

$$\max_{u^*} \lim_{t \rightarrow \infty} x(t),$$

617  
 618

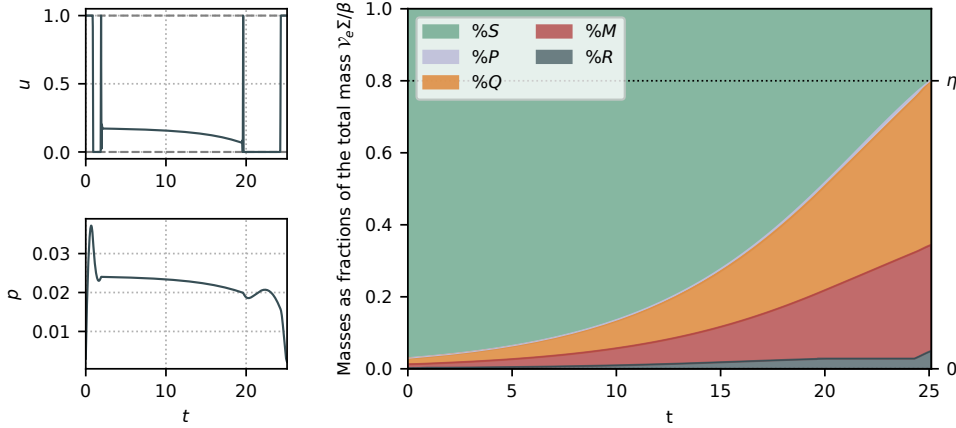


FIG. 8. Numerical simulation of (PP-OCP) with initial conditions  $s_0 = 0.1$ ,  $p_0 = 0.003$ ,  $r_0 = 0.1$  and  $\mathcal{V}_0 = 0.003$ . The performance parameter is fixed to  $\eta = 0.8$ , which is achieved in  $t_f = 25.1$ . Quantities in the right plot are shown as fractions of the total mass in the bioreactor  $\mathcal{V}_e \Sigma / \beta$ .

619 which, using (3.3), can be rewritten as

$$620 \quad \min_{u^*} \lim_{t \rightarrow \infty} \mathcal{V}(t)$$

621  
 622 indicating that maximizing the metabolite concentration at infinite time equates to  
 623 minimizing the biomass. While, in the previous section, the conditions (*Full depletion*)  
 624 and (3.2) were sufficient to determine the asymptotic behavior of the system, the pres-  
 625 ence of  $x$  in this particular problem does not allow a similar resolution. An alternative  
 626 approach, in order to better understand the role of cellular composition in the final  
 627 objective, is to study a simplified version of the problem assuming cellular composition  
 628 is at steady state (a common property of bacterial cells during exponential growth).  
 629 We then propose a reduced version of the dynamical system by fixing the ribosomal  
 630 concentration to a constant value  $r^*$ , which reduces the dimension of the model by  
 631 one. Thus, the metabolite maximization problem is solved in terms of the parameter  
 632  $r^*$ , which represents a simpler analysis that can potentially provide an insight into  
 633 the original optimization problem.

634 **5.1.1. Constant ribosomal concentration.** The system with Constant Ribo-  
 635 somal Concentration  $r^*$  writes

$$636 \quad (\text{CRC-M}) \quad \begin{cases} \dot{s} = -w_M(s)(1 - r^*)\mathcal{V}, \\ \dot{p} = w_M(s)(1 - r^*) - \gamma w_R(p)(1 - r^*) - w_R(p)r^*(p + 1), \\ \dot{\mathcal{V}} = w_R(p)r^*\mathcal{V}. \end{cases}$$

637  
 638 It can be seen that the study of the asymptotic behavior of system (S) applies to  
 639 (CRC-M) as the latter is a particular case of the original one (S) with  $r_0 = u^* = r^*$ .  
 640 We then maximize the final product  $x^*$  in terms of the constant ribosomal concentra-  
 641 tion  $r^* \in [r^-, r^+]$ . The latter is given by the expression

$$642 \quad \max_{r^*} \lim_{t \rightarrow \infty} x(t).$$

643

We can see that the quantity

$$z = s + (p + 1)\mathcal{V} + \gamma \frac{1 - r^*}{r^*} \mathcal{V}$$

644 is constant. Thus,

$$645 \quad \mathcal{V}^* + \gamma \frac{1 - r^*}{r^*} (\mathcal{V}^* - \mathcal{V}_0) = \Sigma$$

646  
647 which, using (3.3), yields

$$648 \quad x^* = \gamma \frac{1 - r^*}{r^*} (\mathcal{V}^* - \mathcal{V}_0).$$

650 Using the fact that  $\mathcal{V}^* + x^* = \Sigma$  from (3.3), we see that  $x^*$  is monotone decreasing w.r.t.  
651  $r^*$ , and so the ribosomal concentration maximizing the infinite-time metabolite mass  
652 is  $r^* = r^-$ . This is what one would expect intuitively in an infinite-time horizon, as  
653  $r^* = r^-$  favors the production of metabolic proteins  $M$ , which catalyzes the synthesis  
654 of metabolites  $X$  without arresting the production of biomass (given by the case  
655  $r^* = 0$ , which cannot be attained in trajectories starting in  $\Gamma$ ). However, this kind  
656 of strategies might perform sub-optimally for the finite horizon case, as not having  
657 enough biomass can translate into a slow metabolite synthesis rate. Mathematically,  
658 this is represented through the presence of  $\mathcal{V}$  in the dynamical equation of  $x$ . Similar  
659 to previous results [27], a first phase dedicated to bacterial growth can also foster  
660 the production of  $X$ , which depends directly on the concentration of bacteria in the  
661 bioreactor.

## 662 5.2. Finite-time problem.

663 **5.2.1. Problem formulation.** In this section, we study the metabolite produc-  
664 tion objective in (S) for a time interval  $[0, t_f]$ , in which the final concentration of  
665 metabolite in the bioreactor  $x(t_f)$  is maximized. While the biomass maximization  
666 objective  $\mathcal{V}(t_f)$  was already studied in model (WTB-M) (representing a wild-type  
667 bacteria), it is likely that the presence of the heterologous pathway responsible for  
668 the production of  $x$  might affect the results already obtained. Thus, the two objec-  
669 tives are compared in model (S) from a numerical perspective. Given a fixed final  
670 time  $t_f > 0$ , the OCP maximizing  $c\mathcal{V}(t_f) + (1 - c)x(t_f)$  (with  $c = \{0, 1\}$  depending  
671 on the objective) with initial conditions (IC) writes

$$672 \quad \text{(MP-OCP)} \quad \left\{ \begin{array}{l} \text{maximize} \quad c\mathcal{V}(t_f) + (1 - c)x(t_f), \\ \text{subject to} \quad \text{dynamics of (S)}, \\ \quad \quad \quad \text{initial conditions (IC)}, \\ \text{and} \quad u(\cdot) \in \mathcal{U}, \end{array} \right.$$

673  
674 It should be noted that the OCP is only valid for  $c = 0$  (representing the metabolite  
675 production objective) and  $c = 1$  (for the biomass maximization objective), and thus  
676 the intermediate values  $c \in (0, 1)$  are not considered. One can easily see that, given  
677 the dynamics of the system, applying PMP would yield a Hamiltonian linear in the  
678 control for both values of  $c$ , which means that the solution of (MP-OCP) is similar to  
679 that of (BM-OCP), given by expression (4.1). However, (MP-OCP) has an additional

680 level of complexity in comparison with (BM-OCP), produced by the presence of  $x$  in  
 681 the model, as well as the term  $-\gamma w_R(p)(1-r)$  in  $\dot{p}$  responsible for the consumption  
 682 of resources for metabolite production. Thus, it was not possible to perform a study  
 683 of the OCP using PMP. A numerical analysis of these results is provided in the next  
 684 section.

685 **5.2.2. Numerical simulations.** The optimal trajectories were obtained follow-  
 686 ing the same procedure as in the biomass maximization case. Figures 9, 10 and 11 are  
 687 solutions of (MP-OCP) where the objective is the final-time product maximization  
 688  $x(t_f)$  (obtained by fixing  $c = 0$ ) for different final times  $t_f$  (40, 60 and 80, respec-  
 689 tively) and with the same set of initial conditions. The metabolite synthesis rate is  
 690 set to  $\gamma = 0.5$ . As expected, and similar to the results obtained for (BM-OCP), the  
 691 optimal control takes the value  $u = 0$  for most of the interval, representing an alloca-  
 692 tion strategy that promotes the synthesis of proteins of the metabolic machinery  $M$ ,  
 693 consequently catalyzing the absorption of nutrients from the medium and the produc-  
 694 tion of  $x$ . Solutions are characterized by a short  $u = 1$  bang arc at the beginning of  
 695 the process, followed by a marginal singular arc before the final  $u = 0$  bang arc. The  
 696 latter suggests that a valid sub-optimal approximation of the optimal control could  
 697 be a simple bang-bang (1-0) control law. In that case, the only degree of freedom  
 698 would be the switching time between bang arcs, that can be easily computed through  
 699 numerical optimization methods. Additionally, and as it can be seen across Figures 9,  
 700 10 and 11, these results do not depend on the final time  $t_f$ : the final bang  $u = 0$  of the  
 701 optimal control is always predominant in the control strategy, and becomes larger as  
 702  $t_f$  increases. The finite-time numerical results are consistent with the results obtained  
 703 for the infinite-time case in Section 5.1.1, in which the ribosomal sector of the cell  $r$   
 704 should be minimized to maximize the production of  $x$ . Figure 12 shows an optimal  
 705 trajectory solution of (MP-OCP) with cost function  $\mathcal{V}(t_f)$ . In this case, the allocation  
 706 strategy is described by an initial bang  $u = 1$  followed by a singular arc that takes up  
 707 most of the optimal solution, with values near to an intermediate strategy  $u = 0.5$ ;  
 708 and a short bang  $u = 0$  at the end. Such strategy leads to a bacterial composition  
 709 much more balanced between ribosomal and enzymatic proteins, in opposition to the  
 710 metabolite production case (with  $c = 0$  for (MP-OCP)), where most of the bacterial  
 711 proteins were dedicated to the metabolic machinery. The latter behavior illustrates  
 712 a natural trade-off between two opposed strategies: maximizing the number of ribo-  
 713 somes to prioritize the synthesis of macromolecules over the production of  $x$  and, at  
 714 the same time, maximizing the enzymatic activity in order to consume the substrate  
 715 in the medium as fast as possible, towards (*Full depletion*).

716 Under the hypothesis that the mechanisms behind the allocation of cellular re-  
 717 sources in bacteria have been optimized to outgrow competitors, it is coherent to  
 718 think that a genetically modified bacteria (e.g. able to synthesize the metabolite  
 719  $X$ ) would also maximize biomass. Thus, these internal mechanisms would produce  
 720 a cellular composition profile similar to the one shown in Figure 12. Indeed, this is  
 721 expected to happen even for artificially engineered specimens, as, in microorganisms,  
 722 natural selection occurs very rapidly (even for time windows in the order of hours)  
 723 due to the strong genetic variability of bacteria and their astonishingly high doubling  
 724 rate. Then, interfering with this strategy so as to obtain allocations maximizing the  
 725 production of metabolites in the bioreactor (as the ones shown in Figures 9, 10 and  
 726 11) can be accomplished by externally shutting down the production of ribosomes at  
 727 a certain time instant, which can be triggered by well-known biotechnological control  
 728 techniques such as growth arrest [11].

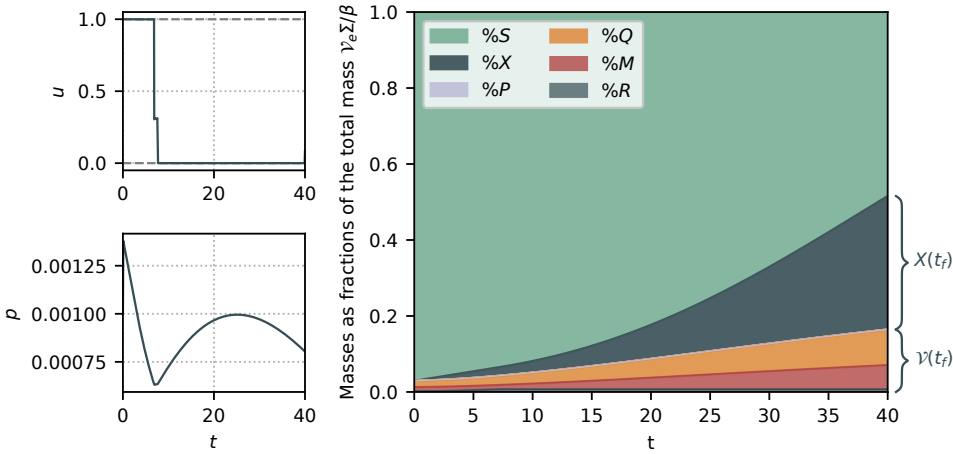


FIG. 9. Solution of (MP-OCP) for the metabolite maximization case  $x(t_f)$ , with  $s_0 = 0.1$ ,  $p_0 = 0.001$ ,  $r_0 = 0.1$ ,  $\mathcal{V}_0 = 0.003$  and  $t_f = 60$ . The final product concentration  $x(t_f)$  is at 35% of the total mass in the bioreactor  $\mathcal{V}_e \Sigma / \beta$ , while the final volume  $\mathcal{V}(t_f)$  is only at 16%.

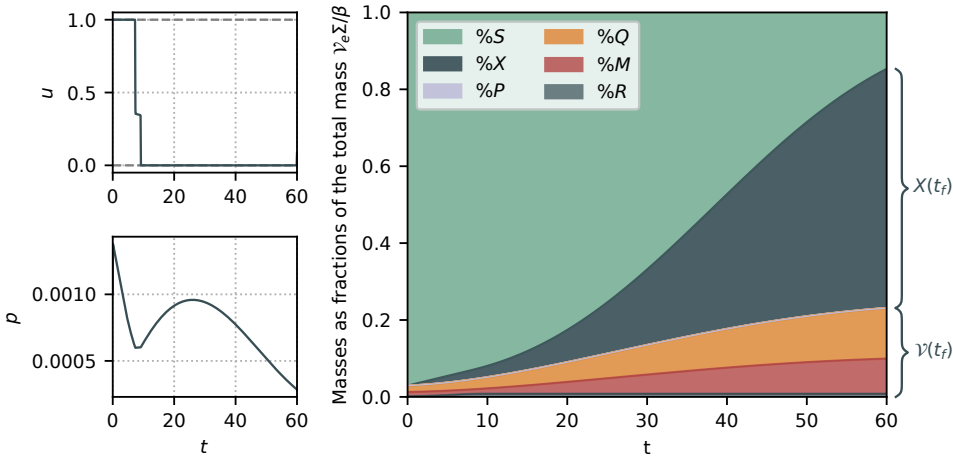


FIG. 10. Solution of (MP-OCP) for the metabolite maximization case  $x(t_f)$ , with  $s_0 = 0.1$ ,  $p_0 = 0.001$ ,  $r_0 = 0.1$ ,  $\mathcal{V}_0 = 0.003$  and  $t_f = 60$ . The final product concentration  $x(t_f)$  is at 62% of the total mass in the bioreactor  $\mathcal{V}_e \Sigma / \beta$ , while the final volume  $\mathcal{V}(t_f)$  is only at 23%.

729 **6. Discussion.** This paper presented a mathematical study of bacterial resource  
 730 allocation in batch processing, and its applications to biomass and metabolite pro-  
 731 duction. A dynamical model considering the production of a value-added chemical  
 732 compound is proposed, and a study of the asymptotic behavior of the system based on  
 733 mass conservation laws shows that, under all possible resource allocation strategies,  
 734 all the substrate in the medium is consumed. Then, the particular case of a wild-type  
 735 bacteria with no metabolite production is analyzed, showing that the optimal allo-  
 736 cation propitious for biomass maximization—and thus, competitors outgrowing—is  
 737 accomplished through a rather low value of the optimal control  $u$ , which yields a very  
 738 high  $m/r$  ratio (i.e. the ratio of enzymatic to ribosomal mass fractions) in the cell



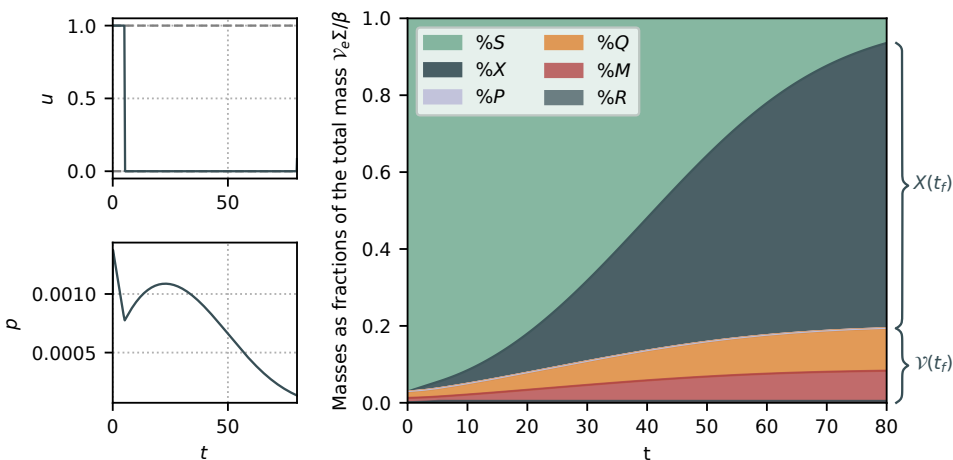


FIG. 11. *Solution of (MP-OCP) for the metabolite maximization case  $x(t_f)$ , with  $s_0 = 0.1$ ,  $p_0 = 0.001$ ,  $r_0 = 0.1$ ,  $\mathcal{V}_0 = 0.003$  and  $t_f = 60$ . The final product concentration  $x(t_f)$  is at 74% of the total mass in the bioreactor  $\mathcal{V}_e \Sigma / \beta$ , while the final volume  $\mathcal{V}(t_f)$  is only at 19%.*

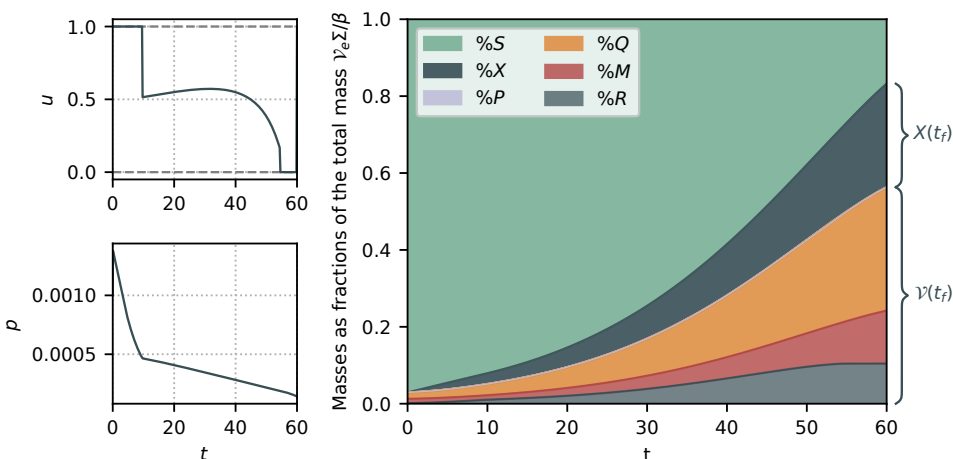


FIG. 12. *Solution of (MP-OCP) for the biomass maximization case  $\mathcal{V}(t_f)$ , with  $s_0 = 0.1$ ,  $p_0 = 0.001$ ,  $r_0 = 0.1$ ,  $\mathcal{V}_0 = 0.003$  and  $t_f = 60$ . The final product concentration  $x(t_f)$  is at 27% of the total mass in the bioreactor  $\mathcal{V}_e \Sigma / \beta$ , while the final volume  $\mathcal{V}(t_f)$  is at 56%.*

739 throughout the bioprocess. Paradoxically, for the metabolite production case, this  
 740 kind of strategies would rather maximize the production of  $x$ , while for maximizing  
 741 the biomass under the presence of the heterologous pathway, a more balanced cel-  
 742 lular composition is required. Overall, results show that optimal allocation can be  
 743 accomplished through a two-phase control: a first phase of pure bacterial growth ded-  
 744 icated to produce as many ribosomal proteins as possible; followed by a production  
 745 phase where the remainder of the feedstock is used to synthesize the compound of  
 746 interest. While the first phase matches the natural bacterial behavior, the second  
 747 one requires human intervention to arrest the production of ribosomes (by externally

748 setting  $u = 0$ ). The obtained two-phased external control profile is in close agreement  
749 with well-known metabolic engineering techniques used in microbial cell factory [27].

750 The analysis presented in this paper raises interesting questions both from math-  
751 ematical and biological points of view. For instance, it would be worthwhile to further  
752 study the potential presence (or absence) of the turnpike phenomenon in the optimal  
753 control solutions. Depending on the complexity of the OCP, it is often possible to  
754 obtain an analytical proof of the exponential convergence of the singular arc to the  
755 solution of the static OCP [25], and to find an explicit link between the length of the  
756 singular arc and the duration of the bioprocess. From a biological perspective, includ-  
757 ing additional substrates could broaden the approach to represent other well-studied  
758 phenomena observed in bacterial growth. For example, under the presence of differ-  
759 ent nutrients in the culture, bacteria tend to favor (i.e. consume first) those that are  
760 easier to metabolize, which is a phenomenon known as diauxic growth. This behavior  
761 has been extensively studied from an optimal control viewpoint, but without taking  
762 into consideration cellular composition. Formulating more comprehensive dynamical  
763 models and studying their associated OCPs can be instrumental in understanding  
764 natural allocation strategies in microbial growth, and in engineering synthetic control  
765 schemes targeting industrial objectives.

766 **Acknowledgments.** The authors thank Hidde de Jong (Microcosme team, Inria  
767 Grenoble – Rhône-Alpes) for many discussions on the biological context. We also  
768 appreciate the help of Sacha Psalmon and Baptiste Schall, from Polytech Nice Sophia,  
769 for the numerical simulations and the production of the online example in the control  
770 toolbox gallery.<sup>5</sup>

771

## REFERENCES

- 772 [1] A. A. AGRACHEV AND Y. SACHKOV, *Control Theory from the Geometric Viewpoint*, vol. 87,  
773 Springer Science & Business Media, 2013.
- 774 [2] M. BASAN, M. ZHU, X. DAI, M. WARREN, D. SÉVIN, Y.-P. WANG, AND T. HWA, *Inflating*  
775 *bacterial cells by increased protein synthesis*, *Molecular systems biology*, 11 (2015), p. 836.
- 776 [3] V. BORISOV, *Fuller's phenomenon*, *Journal of Mathematical Sciences*, 100 (2000), pp. 2311–  
777 2354.
- 778 [4] J.-B. CAILLAU, W. DJEMA, J.-L. GOUZÉ, S. MASLOVSKAYA, AND J.-B. POMET, *Turnpike prop-*  
779 *erty in optimal microbial metabolite production*, *J. Optim. Theory. Appl.*, 194 (2022),  
780 pp. 375–407.
- 781 [5] E. CINQUEMANI, F. MAIRET, I. YEGOROV, H. DE JONG, AND J.-L. GOUZÉ, *Optimal control of*  
782 *bacterial growth for metabolite production: The role of timing and costs of control*, in 2019  
783 18th European Control Conference (ECC), IEEE, 2019, pp. 2657–2662.
- 784 [6] H. DE JONG, J. GEISELMANN, AND D. ROPERS, *Resource reallocation in bacteria by reengineering*  
785 *the gene expression machinery*, *Trends in microbiology*, 25 (2017), pp. 480–493.
- 786 [7] N. GIORDANO, F. MAIRET, J.-L. GOUZÉ, J. GEISELMANN, AND H. DE JONG, *Dynamical allo-*  
787 *cation of cellular resources as an optimal control problem: novel insights into microbial*  
788 *growth strategies*, *PLoS computational biology*, 12 (2016), p. e1004802.
- 789 [8] R. HEINRICH AND S. SCHUSTER, *The regulation of cellular systems*, Springer Science & Business  
790 Media, 2012.
- 791 [9] S. HUI, J. M. SILVERMAN, S. S. CHEN, D. W. ERICKSON, M. BASAN, J. WANG, T. HWA,  
792 AND J. R. WILLIAMSON, *Quantitative proteomic analysis reveals a simple strategy of global*  
793 *resource allocation in bacteria*, *Molecular systems biology*, 11 (2015), p. 784.
- 794 [10] L. HUO, J. J. HUG, C. FU, X. BIAN, Y. ZHANG, AND R. MÜLLER, *Heterologous expression*  
795 *of bacterial natural product biosynthetic pathways*, *Natural Product Reports*, 36 (2019),  
796 pp. 1412–1436.

---

<sup>5</sup>[ct.gitlabpages.inria.fr/gallery/substrate/depletion.html](https://ct.gitlabpages.inria.fr/gallery/substrate/depletion.html)

- 797 [11] J. IZARD, C. D. G. BALDERAS, D. ROPERS, S. LACOUR, X. SONG, Y. YANG, A. B. LINDNER,  
798 J. GEISELMANN, AND H. DE JONG, *A synthetic growth switch based on controlled expression*  
799 *of RNA polymerase*, *Molecular systems biology*, 11 (2015), p. 840.
- 800 [12] G. JEANNE, A. GOELZER, S. TEBBANI, D. DUMUR, AND V. FROMION, *Dynamical resource*  
801 *allocation models for bioreactor optimization*, *IFAC-PapersOnLine*, 51 (2018), pp. 20–23.
- 802 [13] F. MAIRET, J.-L. GOUZÉ, AND H. DE JONG, *Optimal proteome allocation and the temperature*  
803 *dependence of microbial growth laws*, *NPJ systems biology and applications*, 7 (2021),  
804 pp. 1–11.
- 805 [14] D. MOLENAAR, R. VAN BERLO, D. DE RIDDER, AND B. TEUSINK, *Shifts in growth strategies*  
806 *reflect tradeoffs in cellular economics*, *Molecular systems biology*, 5 (2009), p. 323.
- 807 [15] L. S. PONTRYAGIN, *Mathematical theory of optimal processes*, Routledge, 2018.
- 808 [16] M. SCOTT, C. W. GUNDERSON, E. M. MATEESCU, Z. ZHANG, AND T. HWA, *Interdependence of*  
809 *cell growth and gene expression: origins and consequences*, *Science*, 330 (2010), pp. 1099–  
810 1102.
- 811 [17] M. SCOTT, S. KLUMPP, E. MATEESCU, AND T. HWA, *Emergence of robust growth laws from*  
812 *optimal regulation of ribosome synthesis*, *Molecular Systems Biology*, 10 (2014), p. 747.
- 813 [18] I. S. TEAM COMMANDS, *Bocop: an open source toolbox for optimal control*. <http://bocop.org>,  
814 2017.
- 815 [19] E. TRÉLAT AND E. ZUAZUA, *The turnpike property in finite-dimensional nonlinear optimal*  
816 *control*, *Journal of Differential Equations*, 258 (2015), pp. 81–114.
- 817 [20] A. Y. WEISSE, D. A. OYARZÚN, V. DANOS, AND P. S. SWAIN, *Mechanistic links between cellular*  
818 *trade-offs, gene expression, and growth*, *Proceedings of the National Academy of Sciences*,  
819 112 (2015), pp. E1038–E1047.
- 820 [21] A. G. YABO, *Optimal resource allocation in bacterial growth: theoretical study and applications*  
821 *to metabolite production*, PhD thesis, Université Côte d’Azur, 2021, [https://theses.hal.](https://theses.hal.science/tel-03636842)  
822 [science/tel-03636842](https://theses.hal.science/tel-03636842).
- 823 [22] A. G. YABO, J.-B. CAILLAU, AND J.-L. GOUZÉ, *Singular regimes for the maximization of*  
824 *metabolite production*, in 2019 IEEE 58th Conference on Decision and Control (CDC),  
825 IEEE, 2019, pp. 31–36.
- 826 [23] A. G. YABO, J.-B. CAILLAU, AND J.-L. GOUZÉ, *Optimal bacterial resource allocation: metab-*  
827 *olite production in continuous bioreactors*, *Mathematical Biosciences and Engineering*, 17  
828 (2020), pp. 7074–7100.
- 829 [24] A. G. YABO, J.-B. CAILLAU, AND J.-L. GOUZÉ, *Optimal allocation of bacterial resources in fed-*  
830 *batch reactors*, in 2022 European Control Conference (ECC), IEEE, 2022, pp. 1466–1471.
- 831 [25] A. G. YABO, J.-B. CAILLAU, J.-L. GOUZÉ, H. DE JONG, AND F. MAIRET, *Dynamical analysis*  
832 *and optimization of a generalized resource allocation model of microbial growth*, *SIAM*  
833 *Journal on Applied Dynamical Systems*, 21 (2022), pp. 137–165.
- 834 [26] A. G. YABO AND J.-L. GOUZÉ, *Optimizing bacterial resource allocation: metabolite production*  
835 *in continuous bioreactors*, *IFAC-PapersOnLine*, 53 (2020), pp. 16753–16758.
- 836 [27] I. YEGOROV, F. MAIRET, H. DE JONG, AND J.-L. GOUZÉ, *Optimal control of bacterial growth*  
837 *for the maximization of metabolite production*, *Journal of mathematical biology*, 78 (2019),  
838 pp. 985–1032.